Small-Angle Neutron Scattering of Blends of Cross-Linked and Linear Polystyrene

Robert M. Briber* and Barry J. Bauer

Materials Science and Engineering Laboratory, Polymers Division, National Institute of Standards and Technology, Gaithersburg, Maryland 20899

Received August 6, 1990; Revised Manuscript Received October 9, 1990

ABSTRACT: Small-angle neutron scattering (SANS) has been used to study the scattering function and thermodynamics of blends of linear protonated polystyrene (PSH) and cross-linked deuterated polystyrene (PSD). Two series of samples were synthesized. In both cases the samples were made by dissolving the linear PSH in deuterated (d_8) styrene monomer containing a small amount of divinylbenzene, which was then polymerized to form the PSD network around the linear PSH chains. The samples were all made at a concentration of 50/50 by weight PSD/PSH. A special effort was made to keep the samples single phase so that SANS could be used to study the thermodynamics of the single-phase system and compare it with theory. This entailed working at relatively low cross-link densities (<1 mol % cross-link units). Series 1 is a set of samples with the same cross-link density varying the length of the linear chain. Series 2 is a set of samples containing the same length linear chain varying the cross-link density systematically. By extrapolation of $S(q)$ obtained from SANS using an Ornstien–Zernike plot ($S(q)^{-1}$ versus q^2) to $q = 0$, the zero-angle scattering, $S(0)$, was obtained. $S(0)$ is inversely proportional to the second derivative of the free energy with respect to composition, $\partial^2(\Delta f/kT)/\partial\phi^2$. With the assumption of additivity of the free energies of mixing and elasticity, the portion of the zero-angle scattering due to elasticity is calculated from the scattering. The measured zero-angle scattering can be compared to the scattering calculated from the classical free energy of a swollen network. For the series 1 and 2 samples it was found that the samples could be driven to phase separation by increasing either the length of the linear chain or the network density. In the series 1 samples the zero-angle scattering scaled as $S(0)^{-1} \sim 1/N_b$. In the series 2 samples the zero-angle scattering scaled as $S(0)^{-1} \sim 1/N_c$. In addition, the scattering was found to increase as N_c decreased for the series 2 samples, a behavior opposite to that predicted by combining classical rubber elasticity and mixing theories.

Introduction

Small-angle neutron scattering has been used in recent years to study the thermodynamics of phase separation in linear polymer blends and block copolymer systems of various architectures with much success.[1–6] SANS has been used to elucidate the static structure factor, $S(q)$, in these systems, and the critical divergence of $S(q)$ as the phase-separation transition is approached. In this work we use neutron scattering to study the phase-separation transition in systems where one of the components is cross-linked. Linear polymer chains in networks have been studied in the past under the topic of semiinterpenetrating polymer networks (semi-IPN), but a careful review of this area shows that except for a very few compatible systems[9,10] the systems examined are almost exclusively phase separated. Generally, the phase separation occurs during the polymerization and the systems exhibit a nonequilibrium, kinetically controlled two-phase morphology.[5–7] The emphasis in the work presented here is on single-phase systems and the thermodynamics that control the miscibility of the mixture.

The system studied in this paper is cross-linked deuterated polystyrene (PSD) and linear protonated polystyrene (PSH). This work is related to studies published previously on the poly(vinyl methyl ether) (PVME)/PSD system where we have studied both linear-chain PVME chains in cross-linked polystyrene[11] and networks formed from PVME cross-linked to PSD by radiation.[3] The experiments described in this paper will focus on the effect of varying both the network density and the length of the linear chains incorporated in the network. Varying the network density should allow examination of the effect of changing the elastic free energy of the system while varying the length of the linear chain should perturb the mixing portion of the free energy. Small-angle neutron scattering will be used to determine whether the samples are phase separated or miscible, and, if found to be single phase, the extrapolated zero-angle scattering will be used to compare with theory.

Theory

Classical rubber elasticity based on a Gaussian model for a polymer chain leads to the equation for the free energy of a deformed network to be of the form

$$\frac{\Delta f}{kT} = A\bar{\nu}(\lambda_x^2 + \lambda_y^2 + \lambda_z^2 - 3) - B\bar{\nu}\ln(\lambda_x\lambda_y\lambda_z) \quad (1)$$

where λ_i is the extension in the ith direction, $\bar{\nu}$ is the number of elastically effective chains per unit volume, and A and B are constants. For a swollen network, $\bar{\nu}$ can be written as $\bar{\nu} = \phi/v_a N_c$,[12–15] where ϕ is the volume fraction of the network, v_a is the molar volume of the network monomer unit, and N_c is the average number of monomers between cross-link points. There has been considerable argument in the literature over the value of A and B without a general consensus being reached. The constants A and B are generally taken to be $A = {}^1/_2$ and $B = 2/f$ by Flory,[16] where f is the functionality of the cross-link points in the network, but others have argued for different values[17–21] including James and Guth, who argued for no log term ($B = 0$).[17] For isotropic swelling the transformation $\lambda = (\phi_s/\phi)^{1/3}$ can be used, where ϕ_s is the volume fraction where the network is relaxed (the reference state of the network) and ϕ_s is usually taken as the volume fraction where the network was formed.[21] Assuming additivity for the elastic free energy and the Flory–Huggins free energy of mixing for a polymer blend[22,23] allows one to write down the total free energy for a swollen network (where the solvent is now a linear polymer chain).[11–14] The free energy per unit

volume can then be written as

$$\frac{\Delta f}{kT} = \frac{3A}{\upsilon_a N_c}(\phi_s^{2/3}\phi^{1/3} - \phi) + \frac{B\phi}{\upsilon_a N_c}\ln(\phi/\phi_s) + \frac{(1-\phi)\ln(1-\phi)}{\upsilon_b N_b} + \frac{\chi}{\upsilon_0}\phi(1-\phi) \quad (2)$$

where ϕ is the volume fraction of the network, N_b is the number of monomer units in the linear chain (b component), and χ is the Flory interaction parameter. υ_a, υ_b, and υ_0 are the molar volumes of the network monomer unit, linear chain monomer unit (solvent), and reference volume for the lattice (usually taken as $\upsilon_0 = (\upsilon_a\upsilon_b)^{1/2}$). The coexistence curve is obtained when the chemical potentials of the linear b chains inside and outside the network are equal. The chemical potential of the b chains is given by $\mu_b = \partial(\Delta F/kT)/\partial n_b$ where ΔF is the total free energy of the system and n_b is the number of moles of the linear b chains.[11]

$$\mu_b = \frac{2A\phi_s^{2/3}\phi^{1/3}}{\upsilon_a N_c} - \frac{B\phi}{\upsilon_a N_c} + \frac{\phi}{\upsilon_b N_b} + \frac{\ln(1-\phi)}{\upsilon_b N_b} + \frac{\chi}{\upsilon_0}\phi^2 \quad (3)$$

Because the swollen network is in equilibrium with a phase of pure b chains, eq 3 can be used to calculate the coexistence curve directly (upon setting $\mu_b = 0$) without resorting to solving a set of simultaneous equations involving both μ_a and μ_b as is necessary in polymer blends. For the spinodal line extra care must be taken in calculating $\partial^2(\Delta f/kT)/\partial\phi^2$ in order to correctly account for the effect of fluctuations in composition on the already swollen network.[13-15] If this is done, the equation for the spinodal (and the zero-angle scattering) is given as

$$\frac{\partial^2(\Delta f/kT)}{\partial\phi^2} = \frac{B}{\upsilon_a N_c\phi} + \frac{2A\phi_s^{2/3}}{\upsilon_a N_c\phi^{5/3}} + \frac{1}{\upsilon_b N_b(1-\phi)} - 2\frac{\chi}{\upsilon_0} = \frac{k_n}{S(0)} \quad (4)$$

where k_n is a constant that determines the amount of contrast present and depends on the type of radiation used for the scattering experiment. For SANS $k_n = N_a(b_a/\upsilon_a - b_b/\upsilon_b)^2$ where N_a is Avogadro's number and b_i is the neutron scattering length for the ith molecule in the system. For PSH/PSD $k_n = 4.11 \times 10^{-3}$ mol cm^{-4} molecule. The $\phi^{5/3}$ term in eq 4 is different from that published previously.[11,12] Equation 4 is also sometimes termed the osmotic bulk modulus. The value of χ at the spinodal line, termed χ_s, can be defined by setting eq 4 equal to zero and solving for χ.

$$\frac{\chi_s}{\upsilon_0} = \frac{1}{2}\left[\frac{B}{\upsilon_a N_c\phi} + \frac{2A\phi_s^{2/3}}{\upsilon_a N_c\phi^{5/3}} + \frac{1}{\upsilon_b N_b(1-\phi)}\right] \quad (5)$$

Figure 1 shows a phase diagram calculated for a network with $N_c = 500$, $N_b = 50$, $A = 1$, $B = 1/2$, and $\phi_s = 0.5$. The phase diagram shows the behavior of a network in equilibrium with a bath of linear polymer chains such that upon changing the temperature a system in equilibrium would move along the coexistence curve (the solid line in Figure 1). The coexistence curve gives the composition of the swollen network. Tie lines would run between the coexistence curve and the left-hand axis (pure linear chains). The ordinate is in arbitrary temperature units based on the observation that χ generally has the form $C_1 + C_2/T$.[1-6,24-26] The addition of an elastic component to the free energy causes the phase diagram to be asymmetric. In addition, with the form of the free energy given in eq 1 there is no critical point, with the phase transition being

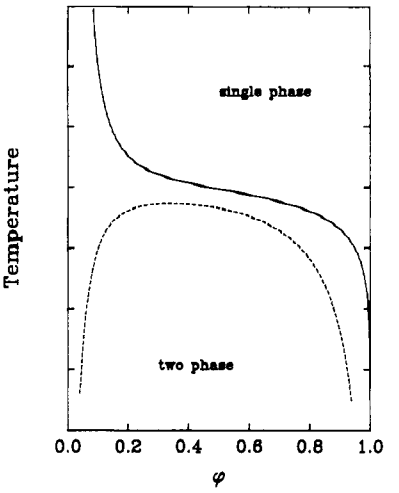

Figure 1. Phase diagram calculated with $N_c = 500$, $N_b = 50$, $A = 1$, and $B = 1/2$. The solid line is the coexistence curve, and the dashed line is the spinodal.

first order at all compositions. Critical points have been observed in network/solvent systems, but usually the presence of the ions adds an additional term to the free energy.[27-30] The scattering from the blends studied in this work is expected to follow classical Ornstein–Zernike form with the total scattering given by

$$S(q) = \frac{S(0)}{1 + (\xi q)^2} \quad (6)$$

where ξ is the correlation length of the concentration fluctuations in the system and q is the scattering vector ($q = (4\pi/\lambda)\sin\theta$).[11,30,31] If the data follow eq 6, then a plot of $S(q)^{-1}$ versus q^2 should be linear, with the correlation length being equal to the square root of the ratio of the slope to the intercept. In analogy with the scattering from linear polymer blends, the intercept of the $S(q)^{-1}$ versus q^2 plot is proportional to the distance from the spinodal line ($\chi_s - \chi$) and the slope is proportional to the square of the average statistical segment length for the system, l_{av}.[2,1-6] For a polymer blend containing two linear polymers, eq 6 can be rewritten as[1]

$$\frac{k_n}{S(q)} = \frac{2}{\upsilon_0}(\chi_s - \chi) + \left[\frac{l_{av}^2/\upsilon_0}{18\phi_a\phi_b}\right]q^2 \quad (7)$$

where

$$\frac{l_{av}^2}{\upsilon_0} = \phi_a\phi_b\left[\frac{l_a^2}{\phi_a\upsilon_a} + \frac{l_b^2}{\phi_b\upsilon_b}\right] \quad (8)$$

Experimental Section

Linear protonated polystyrene (PSH) was purchased from the Pressure Chemical Co. while the deuterated (d_8) styrene monomer and divinylbenzene were purchased from Aldrich.[32] The styrene-d_8 was dried over calcium hydride and distilled. Azobis(isobutyronitrile) (AIBN) was used as the initiator. Samples were prepared by dissolving the PSH in the styrene-d_8 monomer/divinylbenzene mixture. When the PSH was completely dissolved, a few drops of a 10% AIBN solution in toluene was added to give 0.1 wt % initiator. The mixture was then sealed in a SANS cell and placed in a oven at 70 °C overnight. The temperature was then increased to 130 °C for an additional 12 h. The samples were all made at a concentration of 50/50 by weight PSD/PSH. Series 1 is a set of samples with the same network ($N_c = 390$) varying the length of the linear chain ($N_b = 90$, 310, 420, 980, 1700, and 3400). Series 2 is a set of samples containing the same length linear chain ($N_b = 420$) varying the cross-link density systematically ($N_c = \infty$, 960, 480, 340, 260, and 160).

Table I
Series 1 (N_c = 390)

N_b	$S(0)$, cm^{-1}	ξ, Å	$k_n/S(0)$, ×10^5 mol cm^{-3} molecule
90	19.2	26.3	21.4
310	54.0	51.1	76.1
420	95.6	62.6	43.0
980	220	93.6	18.7
1700	1494	263	2.7
3400[a]			

[a] Sample with N_b = 3400 was phase separated.

Table II
Series 2 (N_b = 420)

N_c	$S(0)$, cm^{-1}	ξ, Å	slope[a]	l_{av}, Å	λ	$k_n/S(0)$[b]	$\partial^2(\Delta f/kT)/\partial\phi_{elas}{}^2$ [c]
∞	79.0	51.9	3.37	7.9		5.2	
960	65.9	60.0	3.71	8.3	1.05	4.3	4.4
480	113	66.3	3.82	8.5	1.06	3.6	−61
340	127	93.6	4.78	9.5	1.19	3.2	−101
260	227	111	5.41	10.1	1.27	1.8	−243
160[d]							

[a] Slopes are from the $S(q)^{-1}$ versus q^2 plot ×10^{-1}. [b] ×10^5 mol cm^{-3} molecule. [c] ×10^7 mol cm^{-3} molecule. [d] The sample with N_c = 160 was phase separated.

Tables I and II give the details of the two sets of samples. The cross-link densities were calculated based on the amounts of monomers charged to the reaction and a divinylbenzene activity of 57% as reported by the manufacturer.

The neutron scattering was done at the NIST SANS facility.[32] The wavelength of the incident neutron beam was 9 Å with a $\Delta\lambda/\lambda$ of 25% as determined by a rotating velocity selector. The scattering was performed above T_g at 150 °C. The data were collected by using a two-dimensional x–y detector and were corrected for scattering from the empty cell, incoherent background, and sample thickness and transmission. The scattering was placed on an absolute scale with a calibrated secondary standard. Data were then circularly averaged to obtain the $S(q)$ versus q plots.

Results and Discussion

The two series of samples provide a probe of different parts of the second derivative of the free energy as given in eq 4. If the assumption of additivity of free energies is valid, i.e.

$$\Delta f_{total} = \Delta f_{mix} + \Delta f_{elas} \tag{9}$$

then series 1, where the cross-link density is held constant, while the length of the linear chain is varied, allows examination of Δf_{mix}, specifically the entropic part of the mixing energy. Series 2, on the other hand, keeps the length of the linear chain constant, while N_c varies, thereby probing Δf_{elas}.

Parts a and b of Figure 2 present the SANS data for the series 1 samples as $S(q)$ versus q and $S(q)^{-1}$ versus q^2, respectively. As the length of the linear chain increases, the scattering intensity also increases. In the $S(q)^{-1}$ versus q^2 plot the data form a series of straight lines, which move roughly parallel to each other with progressively smaller intercepts as N_b increases. It was not possible to fit the $S(q)^{-1}$ versus q^2 data for the sample with N_b = 3400 with a positive intercept indicating the sample had phase separated.

Parts a and b of Figure 3 present the SANS data for the series 2 samples. The scattered intensity increases as N_c decreases. The sample with the highest cross-link density (N_c = 160) was phase separated as the data showed significant curvature in the $S(q)^{-1}$ versus q^2 plot and exhibited a negative intercept. The phase separation of this sample can be attributed to the unfavorable contribution to the free energy of the stretching of the network necessary to accommodate the linear chains at this cross-link density. Unlike the data for series 1 samples, the $S(q)$ versus q^2 lines in Figure 3b show a systematic increase in slope with increasing cross-link density.

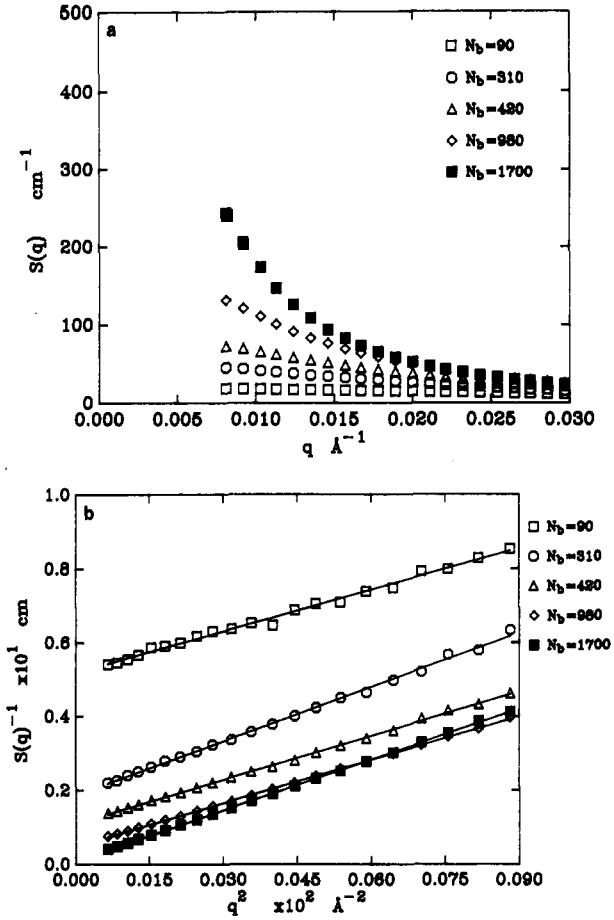

Figure 2. (a) Series 1 samples $S(q)$ versus q SANS data. (b) Series 1 samples $S(q)^{-1}$ versus q^2 data.

Rearranging eq 4 yields

$$\frac{k_n}{S(0)} = \frac{1}{v_b N_b(1-\phi)} + \left[\frac{B}{v_a N_c \phi} + \frac{2A\phi_s^{2/3}}{v_a N_c \phi^{5/3}} - 2\frac{\chi}{v_0}\right] \tag{10}$$

indicating that a plot of $k_n/S(0)^{-1}$ versus $1/v_b N_b(1-\phi)$ should give a straight line with a slope of 1 if the Flory–Huggins combinatorial entropy adequately accounts for the change in the zero-angle scattering brought about by the increase in the length of the N_b chains. Figure 4 is a plot of $S(0)^{-1}$ versus N_b^{-1}. The straight line is a linear least-squares fit to the data and has a slope of 1.03 ± 0.05. The x intercept yields the value of N_b, where $S(0)^{-1}$ = 0, equivalent to an extrapolated spinodal line (where phase separation occurs). The value of N_b for phase separation from Figure 4 is 12 700. This is larger than what is found experimentally for the sample that phase separated (N_b = 3400), but the extrapolation in Figure 4 yields N_b^{-1}, which will give relatively large errors in N_b. Assuming an upper bound value of $\chi/v_0 = 1.5 \times 10^{-6}$ for PSH/PSD,[24,25] the elastic contribution to the second derivative of the free energy can be calculated from the intercept of the line in Figure 4. The value of $\partial^2(\Delta f/kT)/\partial\phi_{elas}{}^2$ is 1.54 × 10^{-5} mol cm^{-3} molecule. The elastic free energy is 1 order of magnitude greater than the enthalpic portion (χ) part of the free energy.

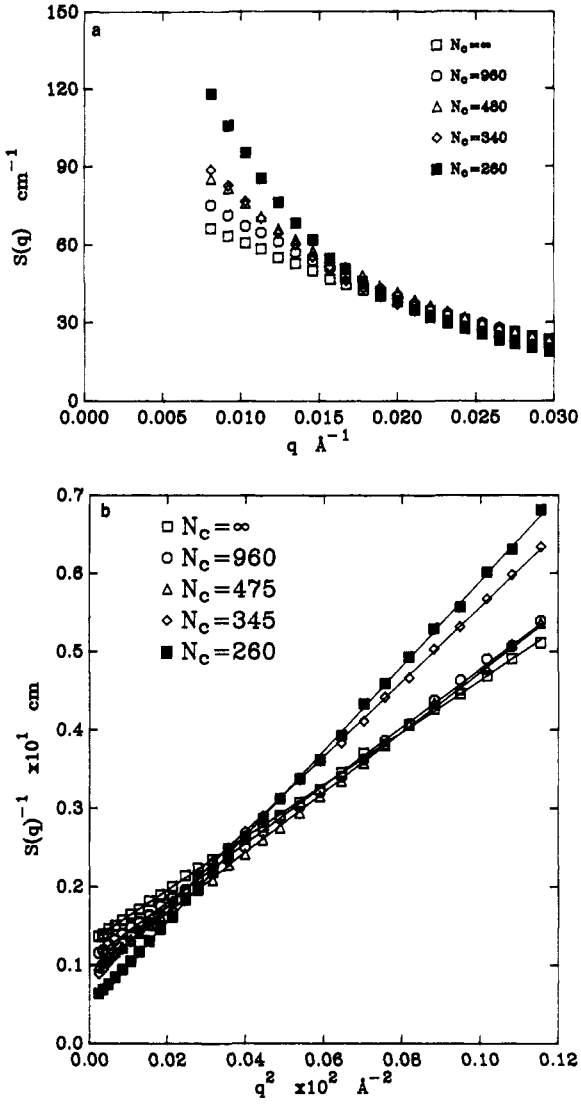

Figure 3. (a) Series 2 samples $S(q)$ versus q SANS data. (b) Series 2 samples $S(q)^{-1}$ versus q^2 data.

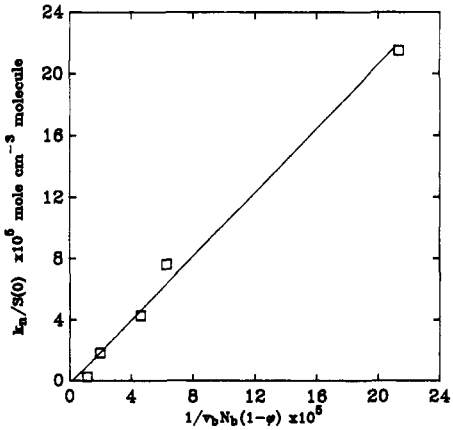

Figure 4. $S(0)^{-1}$ versus $1/N_b$ for the series 1 samples.

For the series 2 samples eq 4 can be rearranged as

$$\frac{k_n}{S(0)} = \frac{1}{v_a N_c}\left[\frac{B}{\phi} + \frac{2A\phi_s^{2/3}}{\phi^{5/3}}\right] + \frac{1}{v_b N_b(1-\phi)} - 2\frac{\chi}{v_0} \qquad (11)$$

and a plot of $k_n/S(0)^{-1}$ versus $1/v_a N_c$ should give a straight line. Equation 11 also assumes that the χ parameter between the PSH chains and the PSD network is independent of the cross-link density. Recent studies have shown that χ can be a function of N_c,[33,34] but the effect

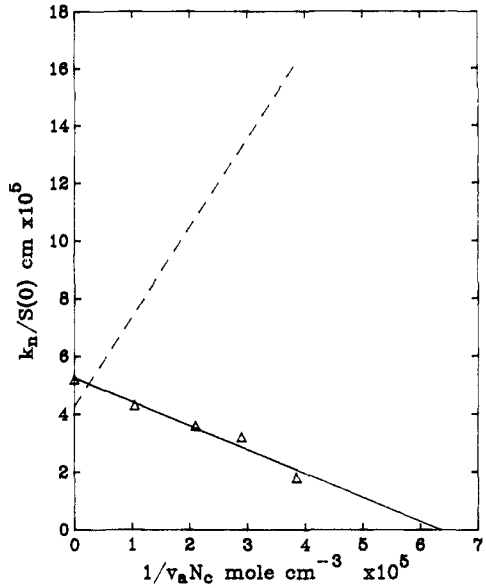

Figure 5. $S(0)^{-1}$ versus $1/N_c$ for the series 2 samples. The dashed line is calculated with eq 11.

should be quite small (10% or less) at the cross-link densities studied in this work. Figure 5 shows such a plot. The solid line is a linear least-squares fit to the data, and the point where it crosses the abscissa is the value of N_c where phase separation occurs ($S(0)^{-1} = 0$). The value of N_c obtained from the extrapolation is 160, in agreement with the value of N_c = 160 where phase separation was observed to have occurred. Equation 11 predicts that the slope of the line in Figure 5 should be positive (the scattering decreasing with increasing cross-link density), which is opposite to what is observed experimentally. The dashed line in Figure 5 is calculated from eq 11. The data and theory do not come together in Figure 5 even at $1/N_c = 0$ because eq 11 neglects the entropic contribution to the scattering from the extra free chains when there are no cross-links present. The differences between theory and experiment will be discussed in more detail later.

Phase separation is observed in both the series 1 and series 2 samples. In neither case can the phase separation be explained only by invoking a positive χ between the PSD and the PSH. In both the series 1 sample (N_b = 3400) and the series 2 (N_c = 160) sample where phase separation occurred, an unfavorable contribution to the free energy from the elastic stretching of the chains drives the system to phase separate.

The correlation length of the concentration fluctuations, ξ, can be calculated from the scattering curves show in Figures 2 and 3 and are given in Tables I and II. For mean-field systems the critical exponent for the divergence of the zero-angle scattering, γ, equals 1, while the exponent for the correlation length $\nu = {}^1/_2$[1-5,31,33] (not to be confused with $\bar{\nu}$, the number of elastically effective chains). The data are plotted as ξ^{-2} versus $1/N_b$ and $1/N_c$ in parts a and b of Figure 6, respectively. The lines through the data are least-squares fit to the data and yield values for phase separation of N_b = 3900 and N_c = 200, in agreement with what is observed experimentally. The fact that the slopes of the $S(q)^{-1}$ versus q^{-2} plots are changing for the series 2 samples indicates that the relationship between $\xi^{-2} \sim 1/N_c$ is not strictly valid but the slope appears to be a relatively weak funciton of N_c compared to ξ. Realistically, one would not expect ξ to diverge to ∞ in systems such as the ones studied in this paper because of kinetic effects. Although the equilibrium phase-separated state is for the network to collapse and "squeeze" out the linear chains,

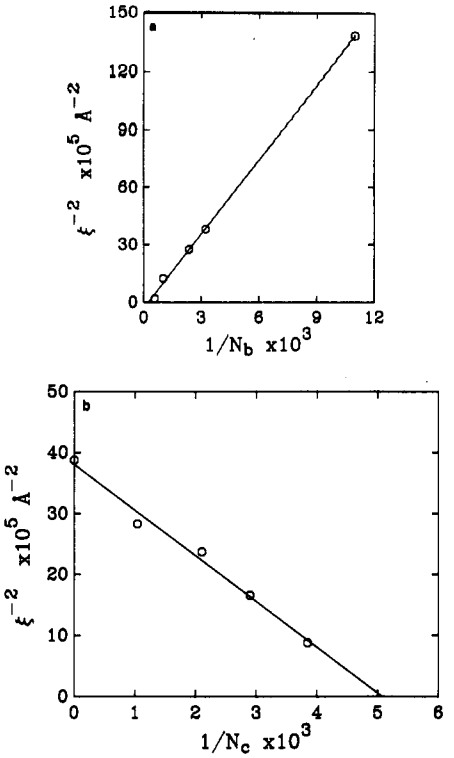

Figure 6. (a) ξ^{-2} versus $1/N_b$ for the series 1 samples. (b) ξ^{-2} versus $1/N_c$ for the series 2 samples.

the observed behavior would undoubtedly be for pockets of material to phase separate locally inside network.

Although there exists no calculation of the full form of $S(q)$ for the systems studied in this paper, we will make the assumption that the slope of the $S(q)^{-1}$ versus q^{-2} is proportional to the square of the statistical segment length, l_{av}^2, as in linear polymer blends. This allows calculation of l_{av} through eq 7. The values of l_{av} for the series 2 samples are given in Table II. The value of l_{av} averaged over all the series 1 samples was 9.0 Å, which is consistent with the series 2 samples. While the value of l_{av} = 7.9 Å for the series 2 sample with $N_c = \infty$ is larger than the literature value of about 6.8 Å for monodisperse polystyrene,[1,36] the molecular weight distribution of the radically polymerized chains would lead to a larger measured value of l_{av}. One possible implication of the dependence of l_{av} on N_c is that either the PSH or the PSD chains (or both) are stretching as N_c decreases. The data cannot distinguish which component might be stretching, but one might speculate that the network chains are forced to stretch in order to accommodate the linear PSH chains. As N_c decreases this stretching increases until the free energy penalty caused by the deformation drives the system to phase separate. The use of eq 7 to calculate l_{av} assumes that the elastic terms in the free energy do not contribute to the q^2 terms in the scattering. We make this assumption because, as mentioned above, of the lack of a calculation of the full form of $S(q)$ for these systems.

The polymerization of the samples studied in this work is quite complex, with the linear chains and partially formed network being swollen by unpolymerized monomer throughout the reaction. During the early stages of the polymerization the chains incorporated in the network could be highly swollen due to the styrene monomer acting as a good solvent, leading to significant residual deformation (and hence an increased value of l_{av}) at the end of the reaction. If one does not worry about the magnitude of l_{av}^2 but examines instead the ratio of the slope of the $S(q)^{-1}$ versus q^2 plot at a given value of N_c to the slope for

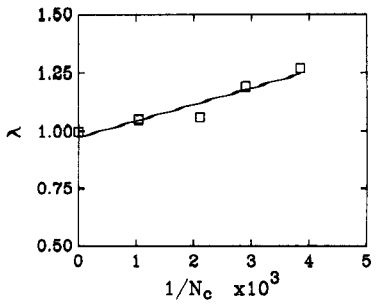

Figure 7. λ versus $1/N_c$ for the series 2 samples.

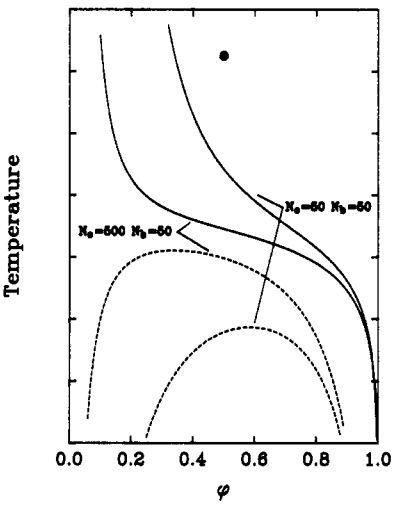

Figure 8. Phase diagram showing coexistence curves and spinodal curves for N_b = 500 with N_c = 500 and N_c = 50.

the un-cross-linked blend ($N_c = \infty$), an estimate of the amount of chain deformation, λ (l_c/l_∞), can be made. The values of λ obtained for the series 2 samples in this manner are given in Table II. Figure 7 is a plot of λ versus $1/N_c$ showing a roughly linear relationship.

One possibility for the difference between the calculated and measured zero-angle scattering shown in Figure 5 arises from the form of the elastic free energy used in calculating the zero-angle scattering. Classical Gaussian rubber elasticity predicts that as the network density increases (N_c decreases) the scattering should decrease. The coexistence curve obtained from eq 3 predicts that the system will swell less at higher cross-link densities. For our experiment with a fixed χ, this translates to the coexistence curve moving closer to the point in the χ,φ plane corresponding to the sample while the calculated spinodal line moves further away (instead of moving closer as the experiments imply). This is shown Figure 8 where the solid lines are the coexistence curves and the dashed lines are the spinodal curves for two different values of N_c. The filled circle near the top of the figure represents a point in the χ,φ plane where an experiment might be done. The curves in Figure 8 are for N_b = 50 with N_c = 500 and N_c = 50 indicating the shift in the phase diagram expected when the length of the linear chain is kept constant and the network density is varied. The spinodal curve moves away from the sample position as N_c deceases, increasing the value of $\chi - \chi_s$ and predicting a decrease in $S(0)$. It remains to be seen whether other theories for network elasticity such as recently proposed by Gaylord and Douglas[37,38] give different results for $S(0)$. Recently Bastide et al. have proposed that the excess intensity observed scattering experiments on swollen networks can be explained by a nonuniform density of cross-links in the sample.[39] While we cannot test this explicitly with our

samples, the difference between theory and experiment also suggests further experiments to confirm this behavior where the relaxed state of the network (ϕ_s) is better defined by performing the polymerization in bulk with the swelling step occurring afterward. Alternatively, model networks swollen with polymeric solvents would provide a useful test of theory. Experiments along these lines are currently planned.

Conclusions

SANS has been used to study the thermodynamics of linear PSH chains in a cross-linked matrix of PSD. Cross-linking, even at low levels, changes the free energy and drives the system toward phase separation. The relatively low levels of cross-linking examined in this work (<1 mol % cross-linking agent) indicate the large effect cross-linking has on the thermodynamics and compatibility in polymer blends, even in miscible systems. Classical Gaussian rubber elasticity theory combined with the Flory–Huggins free energy of mixing has been used to calculate the zero-angle scattering. The prediction is that the scattering should decrease with increasing cross-link density, which is opposite to what is observed. Experimentally it is found that both $S(0)$ and the ξ diverge with decreasing N_c. The scaling behavior $S(0)^{-1} \sim 1/N_c$ was found. For the series 1 samples, where the cross-link density is held constant and the length of the incorporated linear chain is varied, the slope of the plot $S(0)^{-1}$ versus $1/N_c$ is found to be 1.03 ± 0.05, indicating that the Flory combinatorial entropy term successfully describes the data for these samples. In the series 2 samples the slopes of the $S(q)^{-2}$ versus q^{-2} plots increase systematically with decreasing N_c. This can be interpreted as an increase in the average segment step length, l_{av}, with increasing network density. l_{av} is found to vary roughly linearly with $1/N_c$.

References and Notes

(1) Shibayama, M.; Yang, H.; Stein, R. S.; Han, C. C. *Macromolecules* **1985**, *18*, 2179.
(2) Jelenic, J.; Kirste, R. G.; Oberthur, R. C.; Schmitt-Streker, S.; Schmitt, B. J. *Makromol. Chem.* **1984**, *185*, 129.
(3) Briber, R. M.; Bauer, B. J. *Macromolecules* **1988**, *21*, 3296.
(4) Bates, F. S.; Dierker, S. B.; Wignall, G. D. *Macromolecules* **1986**, *19*, 1938.
(5) Han, C. C.; Bauer, B. J.; Clark, J. C.; Muroga, Y.; Matushita, Y.; Okada, M.; Tran-Cong, Q.; Chang, T.; Sanchez, I. C. *Polymer* **1988**, *29*, 2002.
(6) Han, C. C.; Okada, M.; Muroga, Y.; McCrackin, F. L.; Bauer, B. J.; Tran-Cong, Q. *Polym. Eng. Sci.* **1986**, *26*, 3.
(7) Sperling, L. H. *Interpenetrating Polymer Networks and Related Materials*; Plenum: New York, 1981.
(8) Coleman, M. M.; Serman, C. J.; Painter, P. C. *Macromolecules* **1987**, *20*, 226.
(9) Frisch, H. L.; Klempner, D.; Yoon, H. K.; Frisch, K. C. *Macromolecules* **1980**, *13*, 1016.
(10) Boue, F.; Farnoux, B. *Eur. Phys. Lett.* **1986**, *1* (12), 637.
(11) Bauer, B. J.; Briber, R. M.; Han, C. C. *Macromolecules* **1989**, *22*, 940.
(12) Binder, K.; Frisch, H. L. *J. Chem. Phys.* **1984**, *81*, 2126.
(13) Onuki, A. *Phys. Rev. A* **1988**, *38*, 2192.
(14) Onuki, A. In *Formation, Dynamics and Statistics of Patterns*; Kawasaki, K., Ed.; World Science Publishers: Teaneck, NJ, 1989.
(15) Olvera de la Cruz, M.; Briber, R. M., to be submitted for publication.
(16) Flory, P. J. *Principles of Polymer Chemistry*; Cornell University Press: Ithaca, NY, 1953.
(17) James, H.; Guth, E. *J. Chem. Phys.* **1947**, *14*, 669.
(18) Hermans, J. J. *J. Polym. Sci.* **1962**, *52*, 197.
(19) Kuhn, W. *J. Polym. Sci.* **1946**, *1*, 183.
(20) Edwards, S. F. *Proc. Phys. Soc.* **1967**, *92*, 9.
(21) Dusek, K.; Prins, W. *Adv. Polym. Sci.* **1969**, *6*, 1.
(22) Flory, P. J.; Rehner, J., Jr. *J. Chem. Phys.* **1943**, *11*, 521.
(23) Frenkel, J. *Acta Phys. USSR* **1938**, *9*, 235.
(24) Bates, F. S.; Wignall, G. D.; Koehler, W. C. *Phys. Rev. Lett.* **1985**, *55*, 2425.
(25) Yang, H.; Stein, R. S.; Han, C. C.; Bauer, B. J.; Kramer, E. J. *Polym. Commun.* **1986**, *27*, 132.
(26) Olabisi, O.; Robeson, L. M.; Shaw, M. T. *Polymer–Polymer Miscibility*; Academic Press: New York, 1979.
(27) Tanaka, T. *Phys. Rev. A* **1978**, *17*, 763.
(28) Hochberg, A.; Tanaka, T.; Nicoli, D. *Phys. Rev. Lett.* **1979**, *43*, 217.
(29) Tanaka, T.; Fillmore, D.; Sun, S.-T.; Nishio, I.; Swislow, G.; Shah, A. *Phys. Rev. Lett.* **1980**, *45*, 1636.
(30) Ornstein, L. S.; Zernike, F. *Proc. K. Ned. Akad. Wet., Sect. Sci.* **1914**, *17*, 793.
(31) de Gennes, P.-G. *Scaling Concepts in Polymer Physics*; Cornell University Press: Ithaca, NY, 1979.
(32) Certain equipment, instruments, or materials are identified in this paper in order to adequately specify the experimental details. Such identification does not imply recommendation by the National Institute of Standards and Technology nor does it imply the materials are necessarily the best available for the purpose.
(33) Stanley, H. E. *Introduction to Phase Transitions and Critical Phenomenon*; Oxford University Press: New York, 1971.
(34) McKenna, G. B.; Flynn, K. M.; Chen, Y.-H. *Polym. Commun.* **1988**, *29*, 272.
(35) McKenna, G. B.; Flynn, K. M.; Chen, Y.-H. *Macromolecules* **1989**, *22*, 4507.
(36) Brandup, J., Immergut, E. H., Eds. *Polymer Handbook*; Wiley: New York, 1975.
(37) Gaylord, R. J.; Douglas, J. F. *Polym. Bull.* **1987**, *18*, 347.
(38) Gaylord, R. J.; Douglas, J. F. *Polym. Bull.* **1990**, *23*, 529.
(39) Bastide, J.; Leibler, L.; Prost, J. *Macromolecules* **1990**, *23*, 1821.